EC
Journals.ASM.org

Rapid Triacylglycerol Turnover in *Chlamydomonas reinhardtii* Requires a Lipase with Broad Substrate Specificity

Xiaobo Li,[a,b] Christoph Benning,[c] and Min-Hao Kuo[c]

MSU-DOE Plant Research Laboratory, Michigan State University, Lansing, Michigan, USA[a]; Department of Plant Biology, Michigan State University, Lansing, Michigan, USA[b]; and Department of Biochemistry and Molecular Biology, Michigan State University, Lansing, Michigan, USA[c]

When deprived of nitrogen (N), the photosynthetic microalga *Chlamydomonas reinhardtii* accumulates large quantities of triacylglycerols (TAGs), making it a promising source of biofuel. Prominent transcriptional changes associated with the conditions leading to TAG accumulation have been found, suggesting that the key enzymes for TAG metabolism might be among those that fluctuate in their expression during TAG synthesis and breakdown. Using a *Saccharomyces cerevisiae* lipase null mutant strain for functional complementation, we identified the *CrLIP1* gene from *Chlamydomonas* based on its ability to suppress the lipase deficiency-related phenotypes of the yeast mutant. In *Chlamydomonas*, an inverse correlation was found between the *CrLIP1* transcript level and TAG abundance when *Chlamydomonas* cultures were reversibly deprived of N. The CrLIP1 protein expressed and purified from *Escherichia coli* exhibited lipolytic activity against diacylglycerol (DAG) and polar lipids. The lipase domain of CrLIP1 is most similar to two human DAG lipases, DAGLα and DAGLβ. The involvement of CrLIP1 in *Chlamydomonas* TAG hydrolysis was corroborated by reducing the abundance of the *CrLIP1* transcript with an artificial micro-RNA, which resulted in an apparent delay in TAG lipolysis when N was resupplied. Together, these data suggest that CrLIP1 facilitates TAG turnover in *Chlamydomonas* primarily by degrading the DAG presumably generated from TAG hydrolysis.

Plants, animals, and fungi accumulate triacylglycerols (TAGs) to store excess carbon and energy. For industrial biofuel production, triacylglycerol can be converted into fatty acid methyl esters (FAMEs), the major components of biodiesel, through transesterification (12). TAGs harvested from cells can thus be a source of biofuel. Thanks to their higher growth rate and higher oil content, microalgae can, in theory, produce TAG at yields surpassing those of plants (29). However, the details of lipid metabolism in algae are poorly understood.

Chlamydomonas reinhardtii has a long history of serving as a model system for studying cell motility and photosynthesis (18, 31, 41). The recent development of genetic and molecular biological tools, such as nuclear genome transformation (21) and gene silencing with artificial micro-RNA (35), has also made *Chlamydomonas* an excellent model alga for a wider spectrum of research topics, including lipid metabolism and biofuel production. In *Chlamydomonas*, the glycerolipid composition was explored (16), and the lipid metabolism pathways have been annotated *in silico* (38). Certain enzymes for TAG metabolism have also been characterized experimentally (7). Like many other algae, *Chlamydomonas* accumulates TAG under nitrogen deprivation conditions (34, 52).

In plants, TAG biosynthesis starts with the plastid production of fatty acids, which are then esterified to glycerol-3-phosphate, forming phosphatidic acid (PtdOH). The endoplasmic reticulum (ER) is another site for lipid assembly and fatty acid modification (44). Diacylglycerol is produced after the removal of the phosphate group by a PtdOH phosphatase. Diacylglycerol acyltransferases (DGATs) and phospholipid:diacylglycerol acyltransferases (PDATs) then transfer an acyl chain from either an acyl coenzyme A or a phospholipid to diacylglycerol (DAG) to synthesize TAG (53), which can be considered to be a vehicle for carbon storage. TAG turnover (lipolysis) is initiated by the action of TAG lipases, which generate DAG and free fatty acids (13). DAG can be hydrolyzed further into monoacylglycerol and glycerol. Certain lipases hydrolyze all acyl chains from the glycerol backbone, while others may act specifically on one kind of glycerolipid (50). To engineer TAG content, both TAG biosynthetic and hydrolytic enzymes have to be considered. For example, overexpressing an *Arabidopsis* DGAT increases seed oil content (19), whereas deleting the major TAG lipases in the budding yeast *Saccharomyces cerevisiae* results in enhanced accumulation of TAG in cells (4, 5, 24). In *Chlamydomonas*, the functions of two DGATs and a PDAT have been described previously (7, 11, 26). The lipases for the TAG turnover chain reactions have yet to be identified.

As with many other microalgae, *Chlamydomonas reinhardtii* cells do not maintain a large TAG pool during vegetative growth but do so following nutrient deprivation, most notably deprivation of nitrogen (N). Seventy-two hours after N removal, TAG accounts for 50% of all cellular fatty acids, which results from both increased fatty acid biosynthesis and membrane remodeling (33). These metabolic flux changes are accompanied by genome-wide transcription adaptation, including a large number of putative lipase-encoding genes that are up- or downregulated (33). We reasoned that the genes repressed during TAG accumulation may encode lipases that degrade TAG or its initial breakdown products (i.e., diacylglycerol and monoacylglycerol). The N deprivation-induced lipase genes, on the other hand, might be involved in shuffling fatty acids from the membrane lipids to TAG. Here, we describe the identification of a lipase-encoding gene required for rapid TAG turnover in *Chlamydomonas*.

Received 27 September 2012 **Accepted** 27 September 2012
Published ahead of print 5 October 2012
Address correspondence to Min-Hao Kuo, kuom@msu.edu.
Supplemental material for this article may be found at http://ec.asm.org/.

doi:10.1128/EC.00268-12

TABLE 1 Yeast strains used in this study

Strain	Relevant genotype	Source or reference
yMK839	*MATa leu2-3 trp1 ura3-52*	23
yXL001	*MATa leu2-3 trp1 ura3-52tgl4*Δ::*K.l. TRP1*	This study
yXL005	*MATa leu2-3 trp1 ura3-52tgl4*Δ::*K.l. TRP1tgl3*Δ::KanMX	This study
yXL023	*MATa leu2-3 trp1 ura3-52*/pMK595 [2μ *URA3*]	This study
yXL026	*MATa leu2-3 trp1 ura3-52*/pMK595CrLIP1 [2μ *URA3*]	This study
yXL077	*MATa leu2-3 trp1 ura3-52tgl4*Δ::*K.l. TRP1tgl3*Δ::KanMX/pMK595 [2μ *URA3*]	This study
yXL080	*MATa leu2-3 trp1 ura3-52tgl4*Δ::*K.l. TRP1tgl3*Δ::KanMX/pMK595CrLIP1 [2μ *URA3*]	This study

MATERIALS AND METHODS

Yeast methods. Yeast cells were grown according to standard procedures (48). Yeast transformation was performed using the lithium acetate method as described previously (15). The diameters of the yeast cells were determined using the MicroSuite Basic software (Olympus) after microscopy. A uniform lower limit of 4.1 μm for the long-axis cell length was arbitrarily set to exclude young daughter cells. All yeast strains (Table 1) were derived from the yMK839 (23) background, a derivative of the S288C strain. To delete *TGL4*, PCR was done with the primers 4DF and 4DR (all primer sequences are shown in Table S1 in the supplemental material) to amplify *Kluyveromyces lactis TRP1* from pBS1479 (40). The PCR product was then transformed into strain yMK839 for tryptophan prototroph selection to obtain strain yXL001. The deletion was verified by genomic PCR. To delete *TGL3* from yXL001, PCR was performed to amplify the KanMX6 sequence from pFA6a-KanMX6 (51). The PCR product was then gel purified and used as the template for another PCR with the primers 3DF and 3DR. The new PCR product was transformed to yXL001, and the cells were plated onto yeast extract-peptone-dextrose (YPD) with 200 μg/ml G418 for selection, creating yXL005 after genomic PCR verification of the *tgl3*Δ::KanMX allele. In some cases, yeast cells were grown in Casamino Acids (CAA) medium minus uracil (CAA − Ura), which was essentially identical to the synthetic complete medium (48) except for the supplement of 0.5% Casamino Acids and uracil dropout.

To create a cDNA clone for *CrLIP1* expression in yeast, *Chlamydomonas* RNA was prepared with the RNeasy plant minikit (Qiagen). Reverse transcription was conducted with Superscript II reverse transcriptase (Invitrogen) to obtain cDNA. The *CrLIP1* coding sequence was amplified using Phusion polymerase (New England BioLabs) and the primers 595F and 595R. The PCR product was cotransformed into yeast cells together with a NotI-linearized yeast expression vector pMK595 (29) by homologous recombination (30). A single clone of pMK595 with *CrLIP1* integrated (plasmid pMK595CrLIP1) was obtained through transformation of the yeast crude DNA into *Escherichia coli* and sequenced to confirm that it was correct (Table 2). Vector pMK595 and plasmid pMK595CrLIP1 were transformed into strain yMK839 to obtain yXL023 (referred to as *WT-vect* in Fig. 1 and 2) and yXL026 (*WT-CrLIP1*), and into yXL005 to obtain yXL077 (*tgl3*Δ*tgl4*Δ*-vect*) and yXL080 (*tgl3*Δ*tgl4*Δ*-CrLIP1*), respectively.

***Chlamydomonas* strains and growth conditions.** The cell wall-less strain dw15.1 (cw15, nit1, and mt$^+$), obtained from Arthur Grossman (Carnegie Institution, Stanford, CA), was used for all experiments performed on *Chlamydomonas*. The liquid and solid cultures were grown in Tris-acetate-phosphate (TAP) medium as described previously (34). For N deprivation or resupply, the cells were collected by centrifugation at 3,000 × *g* (4°C, 3 min), washed twice, and resuspended in TAP-N (TAP medium with NH_4Cl omitted) or TAP medium, respectively.

TABLE 2 Plasmid constructs used in this study

Plasmid	Main feature	Source or reference
pMK595	2μ*URA3*/P_{ADH1}-3× HA	29
pMK595CrLIP1	2μ*URA3*/P_{ADH1}-3× HA-*CrLIP1*	This study
pMK1006	*ori* Amp^r p*T7*-His6	Unpublished
pMK1006CrLIP1	*ori* Amp^r p*T7*-His6-*CrLIP1*	This study
pChlamiRNA3int	*ori* Amp^r *aphVIII* pPSAD	35
pChlamiRNA3intCrLIP1	*ori* Amp^r *aphVIII* pPSAD-*CrLIP1* targeting oligonucleotide	This study

PCR. Quantitative real-time PCR (qRT-PCR) on *CrLIP1* was performed using the primers qRT-F and qRT-R on the Applied Biosystems 7500 Fast real-time PCR (RT-PCR) system. The data were normalized to the commonly used *RACK1* gene using the primers RACK1-F (receptor for activated C kinase 1 forward) and RACK1 reverse (RACK1-R) (9). The $2^{-\Delta\Delta CT}$ method (28) was employed for data analysis. RT-PCR for the agarose gel electrophoresis was performed using the same primers with the real-time PCR for the *RACK1* and *CrLIP1* genes. For the *DGTT1* gene, the primers DGTT1-F and DGTT1-R were used.

Western blotting. To examine the expression of the *CrLIP1* cDNA in yeast, log-phase yeast cells were collected by centrifugation (3,000 × *g*, 5 min) and then resuspended in 2× SDS-PAGE loading dye (0.12 M Tris-HCl [pH 6.8], 0.04% bromophenol blue, 4% SDS, 20% glycerol, 5.6% β-mercaptoethanol) with the same volume of acid-washed glass beads (0.45 mm; Sigma-Aldrich). The mixture was boiled in a water bath for 5 min followed by 5 min of vortexing. After an additional cycle of boiling and vortexing, the lysates were centrifuged at 21,000 × *g* for 1 min, and the supernatant was analyzed by SDS-PAGE. To examine the subcellular localization of the recombinant CrLIP1 protein, yeast cell pellets were suspended in 0.1 M phosphate-buffered saline (PBS) (pH 7.4) containing the Complete protease inhibitor cocktail (Roche) (one tablet for every 10 ml of buffer). Glass beads (0.45 mm) were added, followed by vigorous agitation in a Mini-BeadBeater (BioSpec) for 45 s and a 1-min incubation in ice. The beating was repeated 3 times. After the last bead beating, the lysates were collected by spinning them through a pinhole punched at the bottom of the tube (1,000 × *g*, 5 min, 4°C). The supernatant of the low-speed spinning was fractionated by 100,000 × *g* centrifugation (90 min, 4°C). The secondary supernatant was defined as the soluble fraction in Fig. 1. The membrane-enriched pellet was suspended in PBS containing the protease inhibitor tablet. For immunoblotting, the 12CA5 monoclonal antibody (Roche) was used to probe for proteins with a hemagglutinin (HA) epitope tag, and the histidine (His) tag monoclonal antibody (catalog no. H1029; Sigma-Aldrich) was used for the hexahistidine-tagged protein in *E. coli*.

Lipid analysis. To extract lipids, *Chlamydomonas* and *E. coli* cells were harvested and resuspended in the lipid extraction solvent containing methanol, chloroform, and formic acid (88%) (2:1:0.1 [vol/vol/vol]). In addition, the bacterial cells expressing *CrLIP1* were shaken at 26°C for 6 h after overnight IPTG (isopropyl-β-D-thiogalactopyranoside) induction before the cells were collected (described below). We found that this extra step allowed for better lipase action in *E. coli*. For lipid extraction, *Chlamydomonas* and *E. coli* cells were vortexed for 30 s in the extraction solvent for cell lysis. For yeast, the cells were resuspended in the solvent, and glass beads (0.45 mm) were added. Yeast lipids were extracted by using a Mini-BeadBeater (BioSpec) as described above for protein preparation, except that 0.5 volume of lipid extraction buffer (1 M KCl, 0.2 M H_3PO_4) was added to the organic phase after its collection by spinning it through a

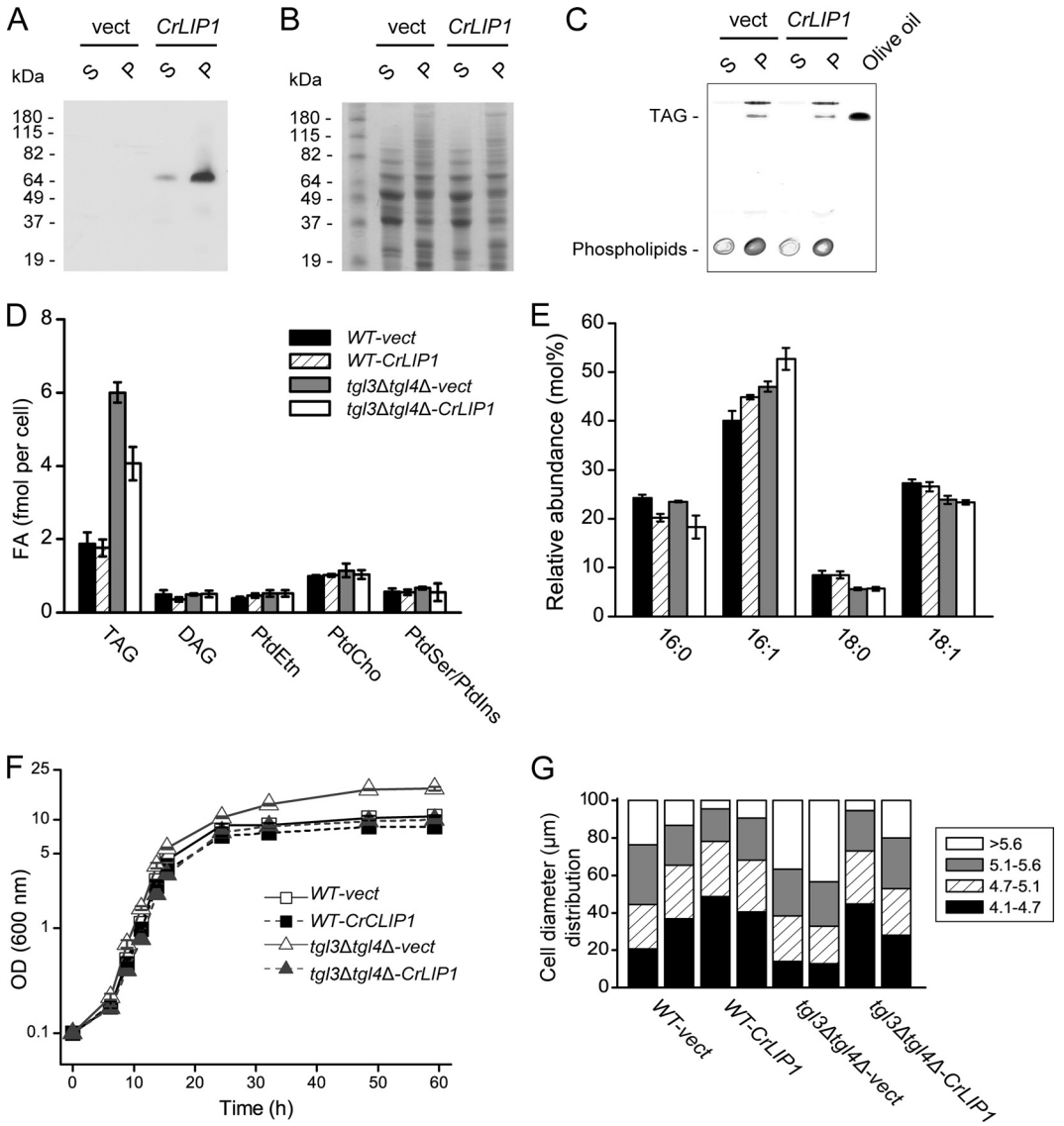

FIG 1 Expression of *CrLIP1* rescues a yeast mutant deficient in TAG lipases. (A) Western blot analysis for HA-tagged CrLIP1 protein expressed in yeast. Whole-cell extracts from *tgl3*Δ *tgl4*Δ mutant yeast cells bearing either the empty pMK595 vector (vect) or pMK595CrLIP1 were centrifuged to obtain a membrane-enriched pellet (P). Ten micrograms of proteins from both the soluble (S) and pellet fractions were loaded for SDS-PAGE before Western blotting (A) or Coomassie brilliant blue staining (B). (C) Thin-layer chromatograph of lipids extracted from membrane-enriched fractions containing 10 μg of proteins. These lipids were visualized by exposing the plate to iodine vapor. (D) Cellular contents of fatty acid (FA) methyl esters derived from major glycerolipids. These lipids were extracted from 2-day-old, stationary-phase yeast cells. Lipid abbreviations: TAG, triacylglycerol; DAG, diacylglycerol; PtdEtn, phosphatidylethanolamine; PtdCho, phosphatidylcholesterol; PtdSer, phosphatidylserine; PtdIns, phosphatidylinositol. (E) Fatty acid compositions of TAG. The fatty acids are designated as a ratio of chain length to the number of double bonds. For panels D and E, averages of three replicates are shown, with errors bars indicating SDs ($n = 3$). (F) Growth curves of yeast strains in uracil dropout medium supplemented with 0.5% Casamino Acids (CAA − Ura). Stationary-phase cells were diluted to an OD_{600} (optical density at 600 nm) of 0.1 to start the time course experiment. Representative results from more than three independent experiments are shown. Data are presented as averages from three measurements of the same culture. Error bars indicate SDs. (G) Distribution of yeast cell diameters in μm (long axis). Cells were grown in uracil dropout medium for 48 h. For each strain, two populations from two single colonies were analyzed. More than 200 cells were measured for each population. The percentages of cells within each size range are shown.

pinhole at the bottom of the tube. For thin-layer chromatography (TLC), lipids were loaded onto silica gel 60 plates (catalog no. 5721-7; EMD Chemicals) and developed in petroleum ether-diethyl ether-acetic acid (80:20:1 [vol/vol/vol], to separate neutral lipids) or chloroform-methanol-acetic acid-H_2O (75:13:9:3 [vol/vol/vol/vol], for the separation of polar lipids). Lipids were visualized by exposure to iodine vapor. For the quantification of fatty acid methyl esters derived from a certain lipid species on the TLC plate, the corresponding spots were scraped and subjected to transesterification and gas-liquid chromatography (GLC) as described previously (43).

Yeast metabolic labeling. To measure the rate of lipid synthesis, yeast cells were grown in CAA − Ura medium for 48 h at 26°C to early stationary phase. To each 5-ml culture, 20 μCi [^{14}C]acetate (specific activity, 45 to 60 mCi/mmol; Perkin Elmer) was added. The cultures were then continually shaken (approximately 150 rpm in a Lab-Line floor incubator) at 26°C and were harvested 25 min, 40 min, 65 min, 100 min, and 140 min

after acetate supplementation. Total lipids were extracted (see above) and resolved by TLC resolution (petroleum ether-diethyl ether-acetic acid, 80:20:1 [vol/vol/vol]) that separated neutral lipids. TAG, DAG, and TLC origins (containing a mixture of polar lipids) were isolated for radioactivity measurement by liquid scintillation counting. For yeast cellular TAG hydrolysis analyses, 50 μCi (0.83 to 1.11 μmol) [^{14}C]acetate was added to 5-ml cultures grown for 48 h at 26°C. After 4 h of labeling, the cells were collected by centrifugation, washed with fresh medium, and diluted 28-fold with fresh CAA − Ura medium to an optical density at 600 nm (OD_{600}) of 0. 4 to 0.6. The cells were shaken for another 5 h with aliquots frozen at each time point. The growth curves were determined with cells grown under exactly the same conditions except that 1 μmol nonlabeled acetate was used. Lipid analysis was performed as described above for lipid synthesis rate analysis.

Recombinant protein production. The *CrLIP1* coding sequence was amplified using the primers ligation-independent cloning forward (LICF) and LIC reverse (LICR) and the Phusion polymerase. The PCR product was then integrated into expression vector pMK1006 through ligation-independent cloning (3). *E. coli* strain BL21-CodonPlus (Stratagene) transformed with empty vector pMK1006 or pMK1006CrLIP1 was grown to the log phase at 37°C, and protein production was induced by the addition of IPTG to a final concentration of 0.5 mM. After 16 h of shaking at 220 rpm at 16°C, the cells were harvested by centrifugation (6,000 × *g*, 5 min, 4°C). For protein preparation, the cells were collected and suspended in the lysis buffer (20 mM Tris-HCl [pH 7.9], 10% glycerol, 150 mM NaCl, 1 mM dithiothreitol) and subjected to three freeze-thaw cycles, followed by sonication on ice (90 times of alternating 1-s pulses and 0.3-s rests, with 1 min of ice chilling after every 15 cycles; a Branson digital sonicator 250 with 25% energy output was used). The cell extracts were obtained through centrifugation at 21,000 × *g* for 15 min and applied to a nickel-nitrilotriacetate (Ni-NTA) affinity purification column (Qiagen). The CrLIP1 protein was eluted with the lysis buffer supplemented with 200 mM imidazole. A spectrophotometric assay with the Bio-Rad protein assay dye reagent concentrate (catalog no. 500-006 EDU; Bio-Rad) (8) was used to determine protein concentrations.

Lipase assay. For the lipase assay with various substrates, lipids dissolved in organic solvents were dried under a stream of nitrogen gas. The dried lipid was then dissolved in 350 μl of 0.1 M phosphate-buffered saline (PBS) (pH 7.4) containing various concentrations of Triton X-100 (see below) by sonication (Sonicator 3000 with a Misonix microprobe) 6 times for 10 s each (power setting, 1.5). Purified CrLIP1 protein or the same volume of protein storage buffer was added. Fresh dithiothreitol (DTT) was added to the final concentration of 2 mM. The mixture was then vortexed and incubated at room temperature.

For the TAG lipase assay, 10 μCi triolein (specific activity, 30 to 120 Ci/mmol) (PerkinElmer) and 5.6 nmol olive oil were dried and resuspended in 350 μl PBS containing 0.11 mM Triton X-100. The mixture was split into halves, and 18 μg of purified CrLIP1 in 20 μl protein storage buffer was added to one of the aliquots. The mixture was then vortexed vigorously for 5 s and incubated at room temperature for 12 h. We tried multiple other conditions for the assay, with varied amounts of olive oil (0 to 250 nmol), DTT, or supplementation of $CaCl_2$. Emulsifiers, including a phosphatidylcholine-phosphatidylinositol mix and bovine serum albumin (BSA) were also used to replace Triton X-100 without any observable effects on the results. For the DAG lipase assay, 150 nmol diolein (Avanti Polar Lipids) was dried and sonicated as described for TAG, except that 0.53 mM, instead of 0.11 mM, Triton X-100 was used. Eighteen micrograms of purified CrLIP1 was added in 50 μl protein storage buffer. The mixture was then vortexed briefly and incubated at room temperature for 16 h.

For assays containing radioactive polar lipids, *Chlamydomonas* cells were grown to log phase in TAP medium, harvested, and suspended in medium with 30 μCi of [^{14}C]acetate, as mentioned above (final concentration, 20 to 23.3 μM). The cells were harvested after another 4 h of standard growth (see above). Total lipids were extracted and resolved by TLC developed in chloroform-methanol-acetic acid-H_2O (75:13:9:3 [vol/vol/vol/vol]). Individual lipids were visualized by radiography and then scraped off the plate before extraction with chloroform-methanol (1:1 [vol/vol]) from the silica gel. Lipids (35 nmol with total radioactivities of 10,000 to 40,000 dpm) were dried and dissolved as described for TAG. For the lipase assays, the emulsified lipid substrates were divided into halves, with 18 μg purified CrLIP1 added to one set and the same volume of protein storage buffer added to the other set. The mixture was incubated for 12 h at room temperature. To prepare radioactive steryl esters for *in vitro* lipolysis reactions, 1 ml of early stationary-phase *tgl3*Δ*tgl4*Δ*-vect* yeast cells were diluted to 25 ml fresh CAA − Ura medium with an additional 30 μCi of [^{14}C]acetate and grown for 48 h at 26°C. Total lipids were extracted and resolved by TLC as described above. The steryl esters were then isolated from the TLC plate. The assay conditions were the same as those for the lipids derived from *Chlamydomonas* cells, with 35 nmol labeled steryl esters (10,000 dpm) as the substrates. For the assays with phosphatidylcholine (PtdCho), 60 nmol 18:1Δ^9/16:0 PtdCho (Sigma-Aldrich) or 18:1Δ^9/16:0 PtdCho (Avanti Polar Lipids) was dried and dissolved as described for TAG. CrLIP1 (36 μg) was added, and aliquots were flash frozen at 0, 6, and 16 h. The 0-h control was used to verify the intactness of PtdCho. The mixture was incubated for 12 h at room temperature. The background levels of fatty acids carried over with purified CrLIP1 protein were estimated in a control reaction without a substrate lipid supplied and subtracted from the free fatty acids data obtained with a substrate.

All the lipase reactions were quenched by adding 2 volumes of lipid extraction solvent. The lipid products were then analyzed by TLC as described above. For *Rhizopus arrhizus* lipase (Sigma-Aldrich) digestion, 200 μg of the enzyme preparation was used, and the incubation time was shortened to 20 min.

amiRNA construct. The artificial micro-RNA (amiRNA) construct needed to silence *CrLIP1* expression was generated according to reference 35. Briefly, four primers were designed using the MicroRNA Designer protocols (http://wmd3.weigelworld.org/cgi-bin/webapp.cgi?page=Help). The primers were annealed by 5 min of boiling and overnight cooling to form a double-stranded fragment with *CrLIP1*-targeting sequences and overhangs compatible with the SpeI digestion site. This fragment was then integrated into the SpeI-linearized pChlamiRNA3int vector (35) through ligation and transformation. To generate *CrLIP1* knockdown lines, the artificial micro-RNA construct (pChlamiRNA3intCrLIP1) or the empty vector was digested with KpnI (New England BioLabs) and transformed into the dw15.1 *Chlamydomonas* strain using the glass bead transformation method (21). TAP agar containing 10 μg/ml paromomycin was used for selection. The real-time PCR described above was used to screen for lines with reduced mRNA abundance of *CrLIP1*.

Bioinformatics. A BLAST (1) search of the CrLIP1 protein sequence in the human genome was performed on the National Center for Biotechnology Information website (http://blast.ncbi.nlm.nih.gov/). Protein sequences were aligned with the ClustalW2 program (25).

RESULTS

Heterologous expression of *CrLIP1* complemented a yeast mutant deficient in TAG lipase activity. To identify the *Chlamydomonas* lipases involved in TAG turnover, we used a yeast mutant deficient in TAG lipase for functional complementation. In yeast, the major TAG lipases are encoded by *TGL3* and *TGL4* (4, 5, 24). Their deletion results in a hyperaccumulation of TAG in stationary-phase cells. This phenotype can be rescued by an ectopic expression of a mouse adipose triglyceride lipase (24). To choose *Chlamydomonas* candidate genes for a lipase that suppress the yeast lipid overstocking phenotype, putative lipases based on Gene Ontology analyses of the Joint Genome Institute (JGI) *Chlamydomonas* 3.0 database were cross-referenced to our transcrip-

tomic studies of N-replete and -depleted cells (33) and to the data from a lipid droplet proteomics study (34). Eight genes were selected for the initial studies. The respective cDNAs were placed under the control of the constitutive *ADH1* promoter from a yeast high-copy-number plasmid. An N-terminal triple-HA tag was added to the coding sequence. These genes were tentatively named *CrLIP1* through *LIP8* (summarized in Table S2 in the supplemental material). The candidate genes *CrLIP1*, *LIP3*, *LIP5*, *LIP6*, and *LIP8* were successfully cloned and expressed in the *tgl3*Δ *tgl4*Δ double-knockout mutant. Of the five genes tested, *CrLIP1* (protein identification no. 184308 and 519543; JGI *Chlamydomonas* 4.0; also known as FAP12 [36]) (see Discussion) consistently showed reduction of TAG and changes in cell growth (see below). For the remainder of this work, we focused on the *CrLIP1* gene for its role in lipolysis.

We first examined the expression of *CrLIP1* in yeast. As expected for a lipase, the majority of recombinant CrLIP1 was associated with the membrane-enriched fraction that also included lipid droplets and TAG (Fig. 1A to C). Importantly, the TAG overaccumulation phenotype of the *tgl3*Δ *tgl4*Δ mutant (5) was partially suppressed by *CrLIP1* overexpression (Fig. 1D). There was no discernible change in the steady-state levels of DAG or major phospholipids, initially suggesting that CrLIP1 primarily affected the TAG accumulation or hydrolysis found in yeast. Although CrLIP1 did not decrease the TAG content in a wild-type background to a statistically significant level (Fig. 1D), it caused consistent differences in the fatty acid compositions of TAG, in both the wild type and the *tgl3*Δ *tgl4*Δ mutant, with an increase in the relative amount of 16:1 and a decrease in 16:0 (Fig. 1E). This might be due to substrate specificity of CrLIP1 if it is a bona fide lipase. Besides these lipid phenotypes, we also noticed that the *tgl3*Δ *tgl4*Δ mutant grew to a higher optical density (OD) in the stationary phase (Fig. 1F). Overexpressing *CrLIP1* prevented this OD increase. One of the underlying reasons for this phenomenon could be the changes in cell size, as revealed by the measurement of cellular diameter under a light microscope (Fig. 1G). Overall, the double lipase knockout strain had a higher number of large cells than did the wild-type strain. Larger particles should absorb more light, resulting in higher ODs. Overexpressing *CrLIP1* in the *tgl3*Δ *tgl4*Δ background caused the overall cell size distribution to approach that of the wild-type cells. Together, these results demonstrate that the *Chlamydomonas* CrLIP1 protein was able to functionally complement the yeast TAG lipases Tgl3 and Tgl4.

Heterologous expression of *CrLIP1* lowers the rate of TAG biosynthesis in yeast. To explore the role of CrLIP1 in yeast TAG metabolism in a more direct way, metabolic labeling experiments were performed. Stationary-phase cells were chosen, as TAG accumulates when cells enter the stationary phase (45). Additionally, from 48 h to 60 h, the increase in cell numbers was within 4% for all strains tested (Fig. 1F); thus, the cell number during the 2-h labeling period was regarded as constant, permitting us to normalize changes in lipid labeling to cell numbers. The radioactivities incorporated into TAG, DAG, and polar lipids (mainly phospholipids in yeast) were measured (Fig. 2A to C). Consistent with the steady-state lipid analysis results (Fig. 1D), the CrLIP1 protein lowered the rate of TAG accumulation (Fig. 2A), while the effects on polar lipids were relatively minor (Fig. 2B). Interestingly, labeling of DAG increased in the first 90 min after the addition of radioactive acetate and dropped afterward. The incorporation of label into DAG (Fig. 2C) was faster than into TAG (Fig. 2A), consistent with DAG being the precursor for TAG biosynthesis. The expression of *CrLIP1* did not affect the initial DAG labeling but, rather, accelerated its reduction. As the immediate precursor of TAG, DAG labeling reduction likely reflected its conversion to TAG. The faster appearance of label in DAG than in TAG and the decrease of label in DAG after 90 min are consistent with a substrate-product relationship of DAG and TAG. The faster decline of DAG label in the presence of CrLIP1 would be consistent with CrLIP1 being a DAG lipase, which could affect the synthesis of TAGs, as observed. Indeed, *in vitro* experiments (see below) confirmed that CrLIP1 has DAG lipase activity.

When growing out of the stationary phase, yeast degrades TAG to produce precursors supporting multiple cellular functions, including membrane polar lipid biosynthesis and energy consumption (45). To shed light on the function of CrLIP1 in yeast, we employed metabolic pulse-chase labeling. To this end, stationary-phase yeast cells were labeled with radioactive acetate and then transferred to fresh medium without the label. The radioactivities in TAG and total polar lipids were quantified. During the course of the chasing period, all strains showed various degrees (up to about 30%) of increases in the optical density (Fig. 2F), a result of cells undergoing mitosis. To accommodate the differences in cell densities, we measured the radioactivities of TAG and polar lipids over a unit volume (per ml) of all strains and normalized them to the starting counts. During the outgrowth, the label in cellular polar lipids increased, whereas TAG labeling remained constant in the wild-type cells (Fig. 2D and E, open squares). Labeling of DAG was very low at the times tested, consistent with very rapid turnover of the DAG pool following the onset of the chase phase of the experiment. The increases of total radioactivities contained in polar lipids likely resulted from the incorporation of persisting radiolabeled acetate and fatty acids. On the other hand, the total amount of TAG remained steady, which we suggest to be a result of balanced TAG synthesis and hydrolysis. Indeed, in the *tgl3*Δ *tgl4*Δ double lipase knockout strain (Fig. 2D and E, open triangles), the total TAG amount increased drastically. Importantly, consistent with a role in lipolysis, the expression of *CrLIP1* in both the wild-type and yeast lipase null strains caused a reduction in TAG labeling levels when cells emerged out of the stationary phase (Fig. 2D, closed triangles and squares). In addition, the labeling of polar lipids also showed a clear decrease in cells expressing the algal CrLIP1 protein (Fig. 2E). Together, these results strongly suggest a lipolytic function of CrLIP1.

Recombinant CrLIP1 hydrolyzes diacylglycerol, but not triacylglycerol, *in vitro*. To examine the lipase activity of CrLIP1 biochemically, the cDNA of *CrLIP1* was cloned into an *E. coli* expression vector. A hexahistidine-tagged CrLIP1 protein was produced, purified (Fig. 3A), and subjected to TAG hydrolysis assays (Fig. 3B). Purified CrLIP1 ran as a doublet on SDS-PAGE (Fig. 3A). Although the underlying reason for this phenomenon remains unclear, the fact that both bands reacted with the anti-His antibody (see Fig. S1 in the supplemental material) indicates that these two bands are isoforms of CrLIP1, not copurified contaminants. Radioactive triolein supplemented with olive oil was incubated with the purified CrLIP1 protein before TLC analysis of the reaction products. Neither iodine vapor stain (not shown) nor autoradiography showed a detectable production of free fatty acids by CrLIP1 (Fig. 3B). Multiple attempts under various reaction conditions all failed to detect the TAG lipase activity of CrLIP1. We also tried another neutral lipid-steryl ester extracted from

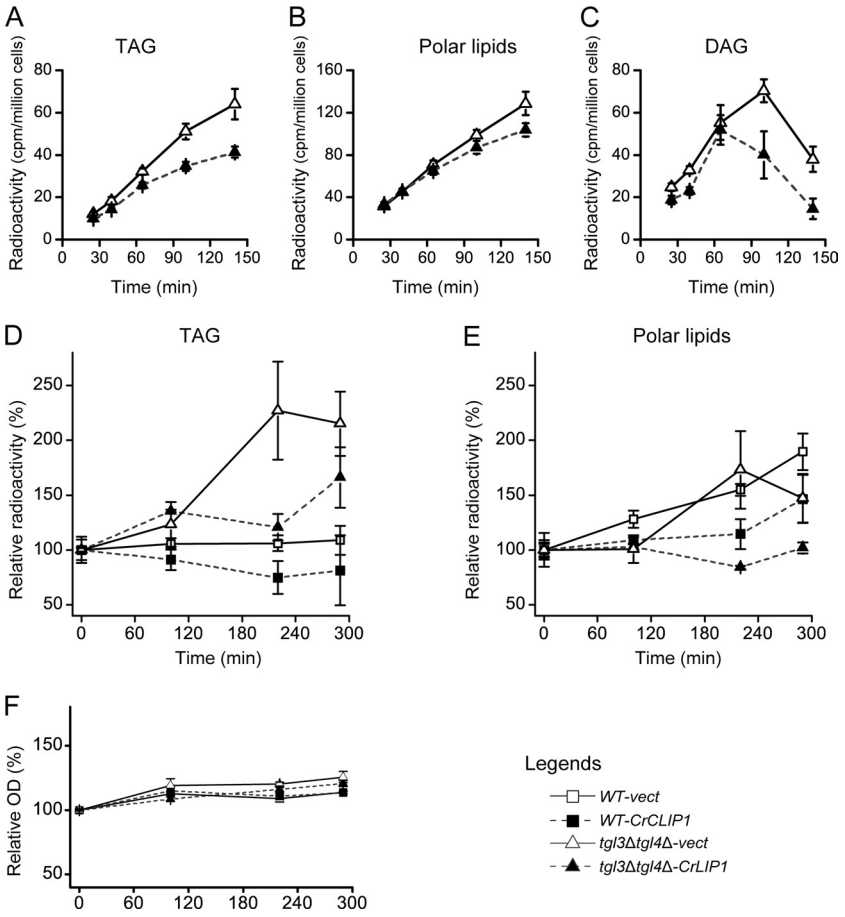

FIG 2 Metabolic labeling and chase studies of TAG and phospholipid synthesis in yeast strains overexpressing *CrLIP1*. [^{14}C]acetate was added to stationary-phase yeast cultures. The samples were taken at the time points indicated, with TAG (A), polar lipids (B), and DAG (C) extracted and quantified. The radioactivities were normalized to the cell number. Data are represented as averages ± SDs ($n = 3$). (D and E) Chase experiments. Stationary-phase yeast cells were labeled, briefly washed, and then diluted in fresh nonlabeled medium. The cells were collected at four time points, with the radioactivities of TAG (D) and polar lipids (E) quantified and normalized to the starting counts. (F) Quantification of cell numbers over the course of the chase experiments. The optical density at 600 nm was measured. For panels D, E, and F, the data are presented as the averages of two technical replicates, with the error bars indicating SDs.

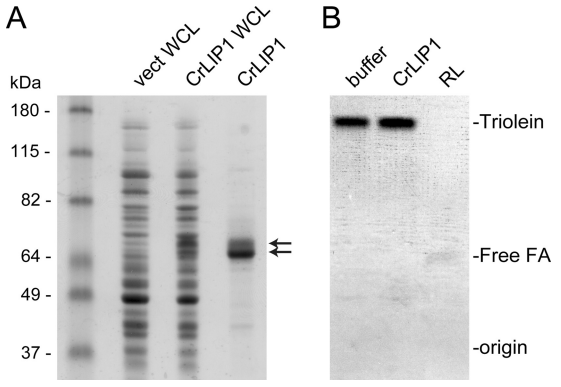

FIG 3 Recombinant CrLIP1 fails to hydrolyze triacylglycerol *in vitro*. (A) SDS-PAGE of bacterial whole-cell lysates (WCL) (6 μg) and purified CrLIP1 protein. Arrows point to two potential isoforms of recombinant CrLIP1. The unlabeled lane shows molecular mass markers. (B) Thin-layer chromatograph of lipids extracted from triacylglycerol lipase assay mixtures with radioactive triolein and olive oil as the substrate. An autoradiograph of TLC is shown. For the buffer-only control lane, the same volume of a CrLIP1 storage buffer was used instead of the purified CrLIP1 protein. *Rhizopus* lipase (RL)-digested triolein was loaded as the marker for free fatty acids.

yeast cells as the substrate and detected no lipolytic activity (see Fig. S2 in the supplemental material).

We had noted that BLAST searches (1) against nonredundant databases revealed considerable similarity between CrLIP1 and the human *sn*-1-specific diacylglycerol lipases DAGLα and DAGLβ (6) (identity scores of 22 with DAGLα and 26 with DAGLβ) (see Fig. S3 in the supplemental material). This prompted us to test the activity of CrLIP1 against DAG. Commercial radiolabeled DAG was not available. To choose a DAG substrate capable of differentiating the reaction products from bacterial fatty acids copurified with the recombinant CrLIP1 protein, we took advantage of the fact that *E. coli* does not synthesize oleic acids (18:1Δ^9) (22); thus, we used diolein [1,2-di(*cis*-9-octadecenoyl)glycerol] as the substrate for *in vitro* lipolysis assays. Reaction mixtures were resolved by TLC, followed by gas-liquid chromatography (GLC) of FAMEs, to identify the fatty acid products. At the position of free fatty acids, there was no visible staining in the absence of CrLIP1 (Fig. 4A), demonstrating that diolein by itself remained intact throughout the entire reaction. In the presence of CrLIP1, on the other hand, iodine staining clearly revealed the production of free fatty acids. Indeed, GLC

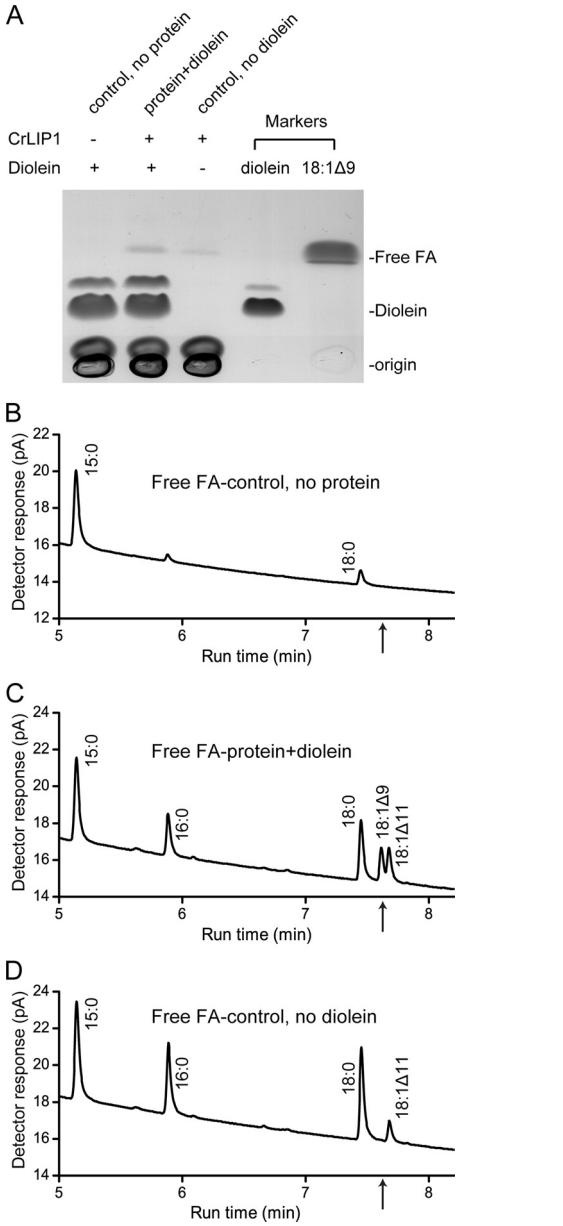

FIG 4 Recombinant CrLIP1 degrades diacylglycerol *in vitro*. (A) Thin-layer chromatograph of lipids extracted from diacylglycerol lipase assay mixtures with diolein as the substrate for CrLIP1. Lane 1, control reaction with diolein and CrLIP1 storage buffer; lane 2, reaction with diolein and purified CrLIP1 protein; lane 3, control reaction with purified CrLIP1 protein without diolein to show fatty acids contained in the protein preparation. Diolein and oleic acid ($18:1\Delta^9$) were loaded as markers. The deep staining at the origins might be from ingredients of the reaction buffer, such as dithiothreitol or glycerol. (B to D) Gas-liquid chromatographs of fatty acid methyl esters (FAMEs) derived from free fatty acids scraped from the TLC plate shown in panel A. Arrows point to the location or expected location of oleic FAME.

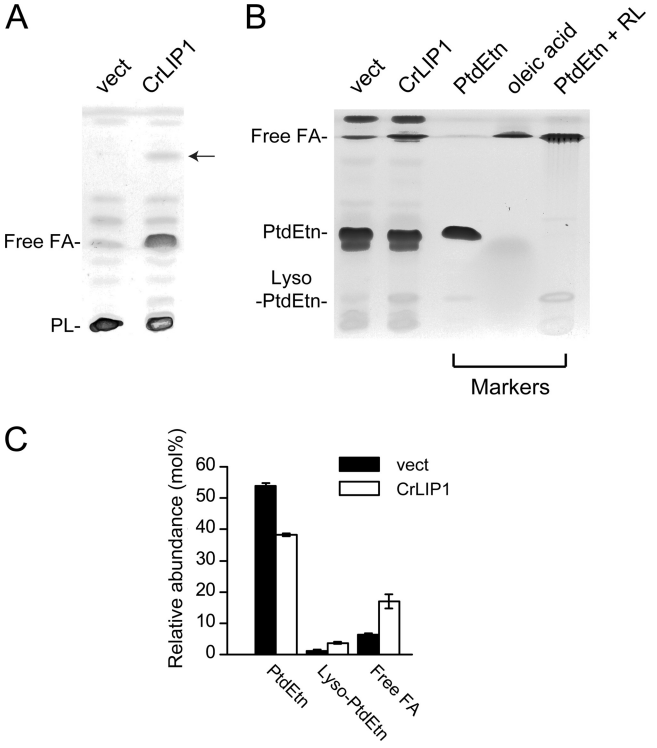

FIG 5 Recombinant CrLIP1 hydrolyzes phosphatidylethanolamine, the major membrane lipid of *E. coli*. (A) Thin-layer chromatographs of total lipids extracted from *E. coli* cells. Note the CrLIP1-dependent production of a significant increase of free fatty acids in the *E. coli* lysate. The arrow points to an unidentified lipid. PL indicates polar lipids. (B) TLC of PtdEtn hydrolysis reactions. The CrLIP1 protein causes the reduction of the PtdEtn substrate and produces free fatty acids and lyso-PtdEtn. The markers include PtdEtn and oleic acid from a commercial source and lyso-PtdEtn generated by the *Rhizopus* lipase (RL). (C) Quantitative analysis of CrLIP1-dependent PtdEtn hydrolysis in *E. coli*. Data are presented as the ratio of fatty acids in each lipid to fatty acids in the total lipid extract. Averages and SDs are shown by the ranges at the tops of the bars in the graph ($n = 3$).

analysis of the free fatty acids isolated from the TLC plate determined unequivocally the presence of oleic acid when CrLIP1 was present in the reaction mixture (Fig. 4C). We thus conclude that CrLIP1 possesses DAG lipase activity.

Recombinant CrLIP1 degrades membrane lipids of *E. coli*. Using *E. coli* crude lysates for the initial testing of the CrLIP1-dependent lipase activity, we noticed a prominent signal of free fatty acids prior to the addition of an exogenous substrate, suggesting that CrLIP1 may have already acted on an abundant bacterial lipid species. To explore this possibility further, we isolated bacterial lipids for TLC analysis and observed the presence of substantial amounts of free fatty acids in the CrLIP1-containing extracts (Fig. 5A). In *E. coli*, phosphatidylethanolamine (PtdEtn) is the most abundant glycerolipid (39), and we suspected that the free fatty acids were at least partly derived from PtdEtn hydrolysis. If so, one of the PtdEtn hydrolysis intermediates, lyso-PtdEtn, might be detectable in the bacterial lipid extracts when CrLIP1 is overproduced. Indeed, when the *sn*-1-specific *Rhizopus arrhizus* lipase (14) was used to generate a standard for lyso-PtdEtn, lyso-PtdEtn increased along with the free fatty acids (Fig. 5B). GLC analyses provided the quantitative support for increases in both free fatty acids and lyso-PtdEtn and PtdEtn reduction in the *CrLIP1*-overexpressing sample (Fig. 5C). These results strongly suggest that CrLIP1 is capable of hydrolyzing glycerophospholipids, such as PtdEtn, which are the major components of biological membranes. Intriguingly, in the neutral TLC on lipids extracted from *E. coli* cells, a new compound (Fig. 5A, arrow) was detected upon *CrLIP1* overexpression. We do not yet know the identity and

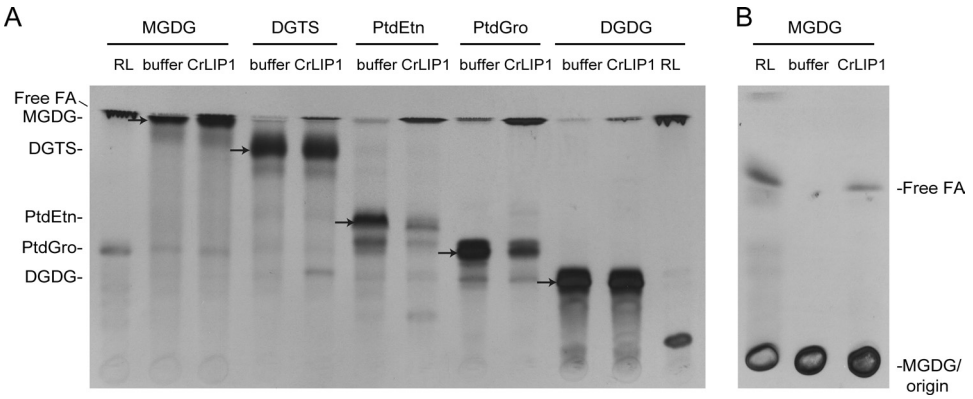

FIG 6 Recombinant CrLIP1 degrades major polar lipids of *Chlamydomonas in vitro*. (A) Thin-layer chromatograph of CrLIP1-catalyzed polar lipid hydrolysis. Each polar lipid was isolated from *Chlamydomonas* cells that were metabolically labeled with [^{14}C]acetate. The positions of the polar lipid substrates are labeled on the left, with arrows near the corresponding substrates. Lipid abbreviations: MGDG, monogalactosyldiacylglycerol; DGTS, diacylglycerol-*N*,*N*,*N*-trimethylhomoserine; PtdGro, phosphatidylglycerol; DGDG, digalactosyldiacylglycerol. Chloroform-methanol-acetic acid-H_2O (75:13:9:3 [vol/vol/vol/vol]) was used to develop the TLC. (B) For a better resolution between the MGDG and free fatty acids, MGDG assay mixtures were loaded onto another TLC, which was developed in petroleum ether-diethyl ether-H_2O (80:20:1 [vol/vol/vol]). MGDG and DGDG digested with *Rhizopus* lipase (RL) were loaded to provide markers for free fatty acids. X-ray films exposed to TLC plates are shown.

origin of this species. While this phenomenon is likely related to the biochemical activity of *CrLIP1*, a definitive identification of this bacterial lipid species will require additional efforts that are beyond the scope of the current work.

Recombinant CrLIP1 hydrolyzes polar lipids. Many lipases, such as the human adipose triglyceride lipase (ATGL) (20) and yeast Tgl4, (37) act on a broad spectrum of glycerolipid substrates. The apparent CrLIP1-dependent lipolysis of PtdEtn in *E. coli* prompted us to explore what other membrane lipids might be substrates for CrLIP1. We focused on abundant *Chlamydomonas* polar lipids that each constituted more than 10% of the membrane lipids: MGDG (monogalactosyldiacylglycerol), DGTS (diacylglycerol-*N*,*N*,*N*-trimethylhomoserine), PtdEtn, PtdGro (phosphatidylglycerol), and DGDG (digalactosyldiacylglycerol). Radiolabeled polar lipids were prepared by growing cells in [^{14}C]acetate-containing medium, since acetate predominantly labels acyl chains rather than the glycerol backbone (46). These substrates would therefore allow us to follow the lipase activity by tracking the production of free fatty acids. The lipolysis reaction products were resolved by TLC and detected by autoradiography. For the five substrates used, lipolysis was documented by the apparent production of radioactive free fatty acids in the presence of CrLIP1(Fig. 6A and B). While CrLIP1 appeared to be more active on phospholipids (i.e., PtdEtn and PtdGro) under the assay conditions, it was difficult to quantitatively determine the substrate preference for these polar lipids, because they were mixtures of molecular species with various specific activities due to the preparation of the substrates by pulse labeling of *Chlamydomonas* cells. Nonetheless, we were able to demonstrate the lipase activity of CrLIP1 against DAG and polar lipids (as shown in Fig. 4 to 6).

Recombinant CrLIP1 hydrolyzes both acyl chains of PtdCho, with a preference for the *sn*-1 position. Diacylglycerol and polar lipids harbor two acyl chains at the *sn*-1 and *sn*-2 positions of the glycerol backbone. Many lipases prefer one position over the other. For example, the lipase from *Rhizopus arrhizus* strongly prefers the *sn*-1 ester bond (14). The human DAGLs also prefer *sn*-1 over *sn*-2, although activities at both positions were detectable (6). To explore the position preference of CrLIP1, we chose phosphatidylcholine (PtdCho) as the substrate. PtdCho is not present in *Chlamydomonas*, but it gave us an opportunity to test a number of commercially available molecular species. Specifically, we used 18:1Δ^9/16:0 (*sn*-1/*sn*-2) and 16:0/18:1Δ^9 PtdCho (Fig. 7). By following the time-dependent liberation of fatty acids from each substrate, the preference (or the lack of preference) for position and/or saturation was observable. Lipase reactions were sampled at 0, 6, and 16 h, and PtdCho, lyso-PtdCho, and free fatty acids were extracted from the corresponding spots on TLC plates for GLC analysis. Only negligible amounts of free fatty acids and lyso-PtdCho were present at 0 h (Fig. 7C and D). After 6 h of incubation, both free fatty acids and lyso-PtdCho emerged, along with a decrease in PtdCho (Fig. 7E and F). For both PtdCho species, fatty acids were mainly, but not exclusively, released from the *sn*-1 position, regardless of the acyl chain. From 6 to 16 h (Fig. 7G and H), the amount of PtdCho remained largely unchanged, whereas the level of lyso-PtdCho decreased, suggesting that CrLIP1 was also able to hydrolyze lyso-PtdCho. Based on these results, we conclude that CrLIP1 prefers the *sn*-1 position but can also hydrolyze the acyl chain at the *sn*-2 position. Moreover, the *sn*-1 oleate and palmitate were mobilized equally well by CrLIP1, suggesting that both oleate and palmitate are comparable substrates for CrLIP1.

Involvement of CrLIP1 in *Chlamydomonas* TAG metabolism. Although we have yet to directly observe TAG lipolysis by using a purified recombinant CrLIP1 protein, it is possible that CrLIP1 is indirectly involved in cellular TAG metabolism. This is because the remodeling of lipids, membrane, and storage is one of the responses to N deprivation that leads to TAG accumulation (33). In addition, DAG is both a precursor and a product (intermediate) for TAG and membrane lipid metabolism (32). The lipase action of CrLIP1 (as shown in Fig. 4 to 7) may impact the flux of DAG and polar lipids, which could eventually affect TAG biosynthesis and breakdown. We took several approaches to test this hypothesis. First, we examined the relationship between changes in the *CrLIP1* transcript and TAG abundance following N deprivation and N resupply. If CrLIP1 plays a role in storage lipid metabolism in *Chlamydomonas* cells, it was expected that the ex-

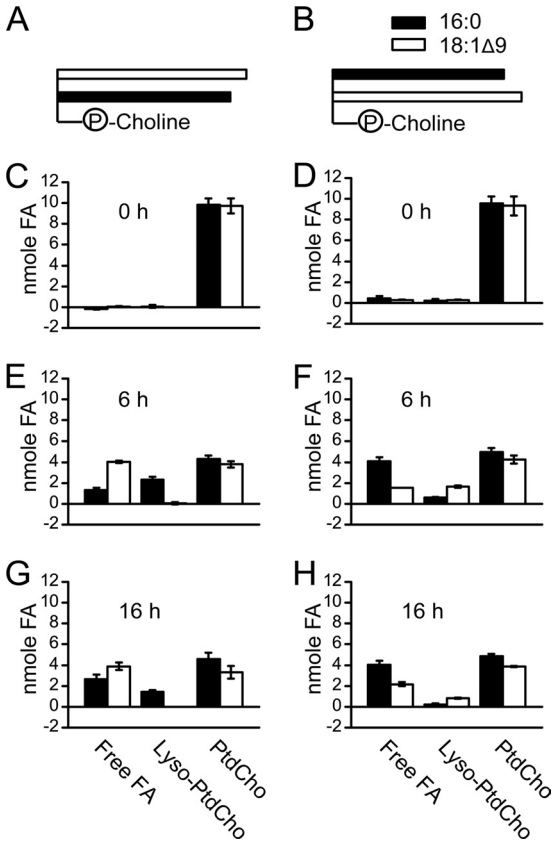

FIG 7 Recombinant CrLIP1 cleaves both acyl groups of phosphatidylcholine with a preference for the *sn*-1 position. (A and B) Schematic representations of the two phosphatidylcholine (PtdCho) substrates. The circled letter "P" denotes phosphate. (C to H) Quantitative analyses of PtdCho lipolysis products. Each lipid species was scraped off the TLC plate, transesterified to FAMEs, and quantified by GLC. Panels C, E, and G represent products derived from 18:1Δ^9/16:0 PtdCho, whereas panels D, F, and H are from the 16:0/18:1Δ^9 PtdCho reactions. Averages and SDs are shown by the ranges at the tops of the bars in the graphs ($n = 3$).

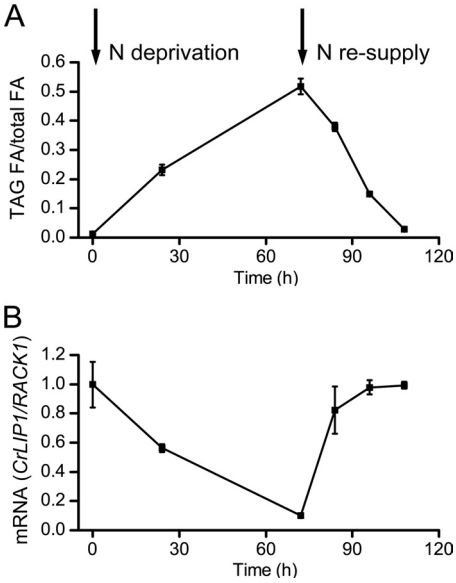

FIG 8 Inverse correlation between *CrLIP1* transcription and TAG abundance in *Chlamydomonas*. (A) TAG abundance through N deprivation and resupply. Data are presented as the molar ratio of fatty acids contained in TAG to total fatty acids in the lipid extract. Log-phase cells were deprived of N for 72 h. After N resupply, the cells were grown for another 36 h. Portions of the cultures at each time point were harvested for lipid and mRNA extraction. (B) *CrLIP1* mRNA abundance from the same cultures examined in panel A. The mRNA was quantified by qRT-PCR. *CrLIP1* transcripts were normalized to the constitutively expressed RACK1, and the *CrLIP1*/*RACK1* ratio at the time of N deprivation initiation was set as 1. In panels A and B, the data are shown as averages ± SDs ($n = 3$).

pression of *CrLIP1* gene would also respond to N fluctuation. *Chlamydomonas* cells started to accumulate TAG shortly after N removal and continued to increase their TAG content (Fig. 8A) (34, 49, 52). N resupply triggered fast TAG mobilization. Consistent with a role in lipolysis, the transcript of *CrLIP1* declined steadily when TAG was accumulating (Fig. 8B). Notably, there was a fast surge of *CrLIP1* transcript that coincided with the N resupply-triggered TAG mobilization. The obvious inverse correlation between the *CrLIP1* transcript level and TAG abundance strongly suggests that CrLIP1 exerts a catabolic function in *Chlamydomonas* TAG metabolism.

To further link *CrLIP1* expression to TAG metabolism, we used an artificial micro-RNA (amiRNA) (35) to reduce the expression of *CrLIP1*. Sixty independent transformants were screened for reductions of *CrLIP1* mRNA levels, and two lines (1-44 and 1-56) exhibited 70 to 80% reductions (Fig. 9A). These two lines and a vector-only control were subjected to N deprivation and TAG quantification. We only observed a slight increase in the TAG levels for the 1-56 line 48 and 72 h into N deprivation (Fig. 9B). The lack of a significant change in the TAG pool size in *CrLIP1* knockdown lines seemed to be in agreement with the N deprivation-dependent decline of *CrLIP1* mRNA; that is, the CrLIP1 lipase activity was likely to be downregulated when TAG synthesis prevailed in the overall energy flux. Knockdown of the *CrLIP1* transcript level thus caused a minimal effect on the total TAG level. On the other hand, when ammonium was added to N-deprived cultures to trigger TAG breakdown, knocking down *CrLIP1* expression resulted in a delay of TAG mobilization. The amounts of TAG normalized to those of total lipids were significantly higher in *CrLIP1* knockdown lines than those in the empty vector controls (Fig. 9C). This phenomenon held true when the TAG content was measured as an absolute amount per cell at 24 h after the resupply of N (Fig. 9D). This observation conforms to a lipolytic role of CrLIP1 *in vivo* and is reminiscent of the slower TAG turnover during postgermination growth of the *sdp1* lipase mutant of *Arabidopsis thaliana* (13). Intriguingly, the maximal TAG amount in the *sdp1* mutant seeds is also indistinguishable from that in the wild-type seeds (13). We thus conclude that the *Chlamydomonas* CrLIP1 plays a critical role in ensuring fast TAG turnover when cells emerge from N deprivation.

DISCUSSION

CrLIP1 affects TAG content possibly by degrading DAG. From the data presented above, we suggest that CrLIP1 affects *Chlamydomonas* and yeast TAG metabolism in different ways. *In vitro*, the recombinant CrLIP1 protein clearly can hydrolyze DAG and phospholipids but not TAG under the standard test conditions. On the other hand, the metabolism of TAG in yeast and in *Chlamydomonas* is affected by changes in the amounts of CrLIP1. Given that DAG is an immediate precursor of TAG synthesis and

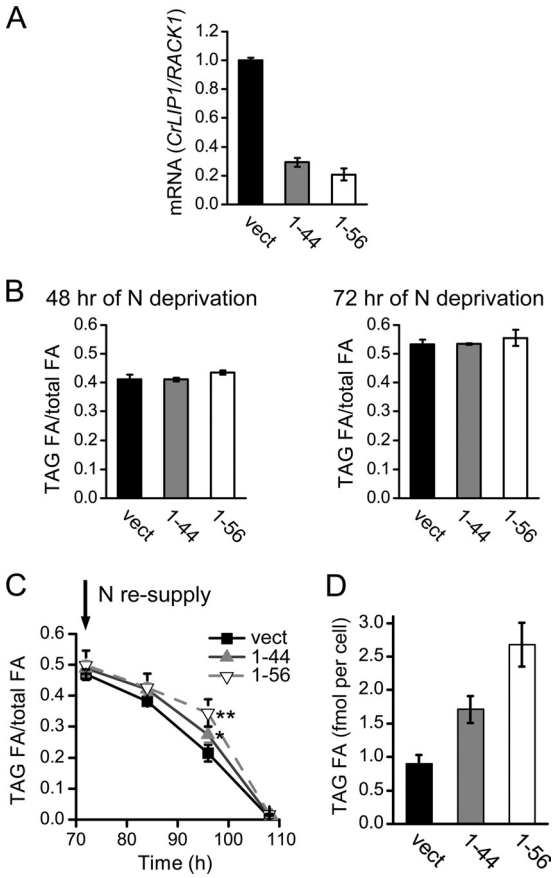

FIG 9 Suppression of *CrLIP1* expression delays TAG turnover in *Chlamydomonas*. (A) Expression of *CrLIP1* in two amiRNA lines compared to an empty-vector control. mRNA quantification was expressed as a *CrLIP1*/*RACK1* ratio and then normalized to the empty-vector control. (B) TAG accumulation at 48 and 72 h of nitrogen deprivation. (C) TAG degradation after the nitrogen resupply described in Fig. 7. (D) TAG amount normalized by cell number 24 h after N resupply to N-deprived cells as described for panel C. Data are shown as averages ± SDs (A, $n = 3$; B, $n = 4$; D, $n = 3$). One asterisk indicates a statistical difference at a P value of <0.05 (t test); two asterisks indicate a statistical difference at a P value of <0.01 (t test).

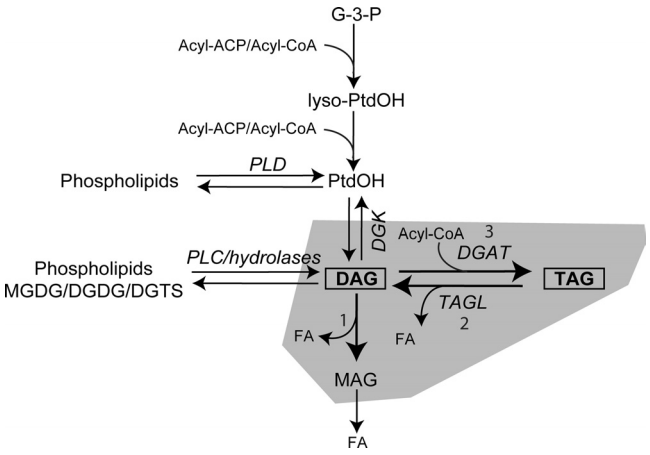

FIG 10 A model for how CrLIP1 might affect TAG metabolism. The DAG lipase activity of CrLIP1 may affect TAG biogenesis and hydrolysis in yeast and *Chlamydomonas*, respectively. Enzymes are italicized. Note that the model stresses components directly related to *CrLIP1* overexpression or knockdown. Not all enzymes or metabolites are shown. Abbreviations for enzymes and lipids: ACP, acyl carrier protein; DGAT, diacylglycerol acyltransferase; DGK, diacylglycerol kinase; G-3-P, glycerol-3-phosphate; PLC, phospholipase C; PLD, phospholipase D; PtdOH, phosphatidic acid; TAGL, triacylglycerol lipase.

an intermediate of TAG degradation, changes in DAG pool sizes will presumably impact TAG abundance in different directions. Accordingly, as shown in Fig. 10, we propose that CrLIP1 participates in TAG turnover in *Chlamydomonas* by facilitating DAG removal during TAG mobilization (Fig. 10, reaction 1), thus contributing to expeditious conversion of TAG into cell building blocks and metabolic energy following the reintroduction of N. The repression of *CrLIP1* expression by artificial micro-RNA may transiently increase the DAG pool, which then delays TAG turnover by-product inhibition through feedback control. The overall rate of TAG hydrolysis is thus reduced. However, possibly due to functional redundancy, or as a result of metabolism of DAG through other routes such as conversion to phosphatidic acid (2), TAG that accumulates following N deprivation eventually will be turned over quantitatively (Fig. 8B). In yeast, the *tgl3*Δ *tgl4*Δ double mutant has no detectable TAG lipase activity (Fig. 10, reaction 2) (24). This argues against the notion that CrLIP1 suppresses the TAG accumulation phenotype solely by expediting DAG removal following the first TAG hydrolysis step, as the lipolytic route of DAG production is blocked by the deletion of TAG lipases. Rather, we suggest two hypotheses. First, yeast gradually accumulates TAG as cells enter the stationary phase (10, 27). The introduction of a heterologous DAG lipase CrLIP1 may result in a shortage of DAG supply for TAG biosynthesis (Fig. 10, reaction 3), partially preventing the TAG-accumulating phenotype seen in the lipase knockout strains. Second, due to the pleiotropic metabolic, as well as the signaling, functions of DAG, the steady-state DAG amount has to be tightly controlled (47). The action of CrLIP1 in yeast may cause alterations in TAG metabolism by an indirect route involving DAG signaling. Nevertheless, we cannot exclude the possibility that CrLIP1 is indeed a TAG lipase *in vivo* but requires an unknown cofactor that was absent in our assay mixtures or a posttranslational modification on the protein that could not be performed in *E. coli* cells.

In addition to phenotypes in TAG metabolism, overexpressing *CrLIP*1 in yeast also affected the rate of polar lipid accumulation in cells emerging from the stationary phase. The observed phospholipid lipase activity (Fig. 5 to 7) can account for the phenotype discussed above, although the stationary-phase cells appear to be relatively insensitive to *CrLIP*1 overexpression (Fig. 1D and 2B). Alternatively, as DAG can be converted to phosphatidic acid and other phospholipids, including PtdEtn and PtdCho (17), CrLIP1 may simply hydrolyze and remove DAG from the pool for polar lipid biosynthesis, thus creating a futile cycle that hampers the rate of polar lipid accumulation.

Is there another function of CrLIP1? In *Chlamydomonas*, *CrLIP1* appears to be actively expressed during vegetative growth when cells maintain a negligible amount of steady-state TAG (Fig. 8, time 0). The qRT-PCR results shown in Fig. 8 are consistent with our earlier work, in which global whole-transcriptome shotgun sequencing (RNA-seq) analysis was employed to examine the transcriptomic changes during N deprivation. The number of *CrLIP1* transcript hits was 2,921 ± 687 under N-replete conditions and were down to 1,335 ± 149 following 48 h of N depriva-

tion (33). Comparatively, the average number of transcript hits for all genes was only 570 during vegetative growth. qRT-PCR verified the abundant *CrLIP1* mRNA when compared with a constitutively expressed *RACK1* gene (see Fig. S4 in the supplemental material). These data demonstrate the active expression of *CrLIP1* during vegetative growth. Assuming that transcript abundance correlates with the protein level, these expression data suggest that CrLIP1 may be a relatively abundant protein during vegetative growth. Given that many *Chlamydomonas* major membrane lipids, such as MGDG and DGDG, are derived from DAG (33) and that CrLIP1 is capable of hydrolyzing DAG and these major *Chlamydomonas* polar lipids, it seems possible that CrLIP1 may be involved in DAG and membrane lipid turnover during mitotic growth when active membrane synthesis and remodeling take place. In contrast, following N deprivation, DAG is synthesized but then channeled into TAG production by DGATs (7). A DAG lipase activity of CrLIP1 would be at odds with the need for cells to accumulate TAG, hence the observed decline of *CrLIP1* transcript following N deprivation. To delineate the potential additional function of CrLIP1 in vegetative cells, the localization of CrLIP1 may have provided some useful information. Unfortunately, our attempts to express a CrLIP1-green fluorescent protein (GFP) fusion protein have not been successful. Intriguingly, CrLIP1 was detected in a flagellum proteomic survey and was designated FAP12 (flagellum-associated protein 12) (36). Thus far, we have not observed a discernible flagellar phenotype associated with either of the CrLIP1 knockdown lines characterized above (data not shown). One possibility is that *CrLIP1* repression in the amiRNA lines was not sufficient to bring about an apparent flagellar phenotype. On the other hand, given the similarity between CrLIP1 and the human DAG lipases DAGLα and DAGLβ that are localized in the plasma membrane (6), it is possible that part of the flagellum-associated CrLIP1 population may have derived from the plasma membrane, as the flagellar membrane is confluent with the plasma membrane (42). Thus, the presence of CrLIP1 in flagella does not contradict our hypothesis of CrLIP1 involvement in TAG metabolism.

CrLIP1 did not exhibit TAG lipase activity under our test conditions, and repressing *CrLIP1* expression delayed, but did not prevent, TAG turnover. Therefore, other TAG lipases in *Chlamydomonas reinhardtii* remain to be identified.

ACKNOWLEDGMENTS

We thank Barbara B. Sears for her critical reading and generous help with techniques involving *Chlamydomonas*, Astrid Vieler and Simone Zäuner for help with lipid analysis, Jianjun Luo and Xinjing Xu for help with yeast genetics and molecular biology, and Dexin Sui for help with recombinant protein purification.

This research was supported in part by a grant from the Gene Expression in Development and Disease (GEDD) focus group to M.-H.K. and C.B. and a grant from the U.S. Air Force Office of Scientific Research to C.B. (no. FA9550-11-1-0264). X.L. received a fellowship from the GEDD.

REFERENCES

1. **Altschul SF, et al.** 1997. Gapped BLAST and PSI-BLAST: a new generation of protein database search programs. Nucleic Acids Res. **25**:3389–3402.
2. **Arisz SA, Testerink C, Munnik T.** 2009. Plant PA signaling via diacylglycerol kinase. Biochim. Biophys. Acta **1791**:869–875.
3. **Aslanidis C, de Jong PJ.** 1990. Ligation-independent cloning of PCR products (LIC-PCR). Nucleic Acids Res. **18**:6069–6074.
4. **Athenstaedt K, Daum G.** 2003. YMR313c/TGL3 encodes a novel triacylglycerol lipase located in lipid particles of *Saccharomyces cerevisiae*. J. Biol. Chem. **278**:23317–23323.
5. **Athenstaedt K, Daum G.** 2005. Tgl4p and Tgl5p, two triacylglycerol lipases of the yeast *Saccharomyces cerevisiae* are localized to lipid particles. J. Biol. Chem. **280**:37301–37309.
6. **Bisogno T, et al.** 2003. Cloning of the first sn1-DAG lipases points to the spatial and temporal regulation of endocannabinoid signaling in the brain. J. Cell Biol. **163**:463–468.
7. **Boyle NR, et al.** 2012. Three acyltransferases and a nitrogen responsive regulator are implicated in nitrogen starvation-induced triacylglycerol accumulation in *Chlamydomonas*. J. Biol. Chem. **287**:15811–15825.
8. **Bradford MM.** 1976. A rapid and sensitive method for the quantitation of microgram quantities of protein utilizing the principle of protein-dye binding. Anal. Biochem. **72**:248–254.
9. **Chang CW, Moseley JL, Wykoff D, Grossman AR.** 2005. The LPB1 gene is important for acclimation of *Chlamydomonas reinhardtii* to phosphorus and sulfur deprivation. Plant Physiol. **138**:319–329.
10. **Clausen MK, Christiansen K, Jensen PK, Behnke O.** 1974. Isolation of lipid particles from baker's yeast. FEBS Lett. **43**:176–179.
11. **Deng XD, et al.** 2012. The roles of acyl-CoA: diacylglycerol acyltransferase 2 genes in the biosynthesis of triacylglycerols by the green algae *Chlamydomonas reinhardtii*. Mol. Plant **5**:945–947.
12. **Durrett TP, Benning C, Ohlrogge J.** 2008. Plant triacylglycerols as feedstocks for the production of biofuels. Plant J. **54**:593–607.
13. **Eastmond PJ.** 2006. SUGAR-DEPENDENT1 encodes a patatin domain triacylglycerol lipase that initiates storage oil breakdown in germinating *Arabidopsis* seeds. Plant Cell **18**:665–675.
14. **Fischer W, Heinz E, Zeus M.** 1973. The suitability of lipase from *Rhizopus arrhizus delemar* for analysis of fatty acid distribution in dihexosyl diglycerides, phospholipids and plant sulfolipids. Hoppe-Seylers Z. Physiol. Chem. **354**:1115–1123.
15. **Gietz D, St. Jean A, Woods RA, Schiestl RH.** 1992. Improved method for high efficiency transformation of intact yeast cells. Nucleic Acids Res. **20**:1425.
16. **Giroud C, Gerber A, Eichenberger W.** 1988. Lipids of *Chlamydomonas reinhardtii.* Analysis of molecular species and intracellular site(s) of biosynthesis. Plant Cell Physiol. **29**:587–595.
17. **Han GS, O'Hara L, Siniossoglou S, Carman GM.** 2008. Characterization of the yeast DGK1-encoded CTP-dependent diacylglycerol kinase. J. Biol. Chem. **283**:20443–20453.
18. **Harris EH, Stern DB, Witman G.** 2009. The *Chlamydomonas* sourcebook: introduction to *Chlamydomonas* and its laboratory use. Academic Press, San Diego, CA.
19. **Jako C, et al.** 2001. Seed-specific over-expression of an *Arabidopsis* cDNA encoding a diacylglycerol acyltransferase enhances seed oil content and seed weight. Plant Physiol. **126**:861–874.
20. **Jenkins CM, et al.** 2004. Identification, cloning, expression, and purification of three novel human calcium-independent phospholipase A2 family members possessing triacylglycerol lipase and acylglycerol transacylase activities. J. Biol. Chem. **279**:48968–48975.
21. **Kindle KL.** 1990. High-frequency nuclear transformation of *Chlamydomonas reinhardtii*. Proc. Natl. Acad. Sci. U. S. A. **87**:1228–1232.
22. **Kito M, Aibara S, Kato M, Hata T.** 1972. Differences in fatty acid composition among phosphatidylethanolamine, phosphatidylglycerol and cardiolipin of *Escherichia coli*. Biochim. Biophys. Acta **260**:475–478.
23. **Kuo MH, Zhou J, Jambeck P, Churchill ME, Allis CD.** 1998. Histone acetyltransferase activity of yeast Gcn5p is required for the activation of target genes in vivo. Genes Dev. **12**:627–639.
24. **Kurat CF, et al.** 2006. Obese yeast: triglyceride lipolysis is functionally conserved from mammals to yeast. J. Biol. Chem. **281**:491–500.
25. **Larkin MA, et al.** 2007. Clustal W and Clustal X version 2.0. Bioinformatics **23**:2947–2948.
26. **La Russa M, et al.** 2012. Functional analysis of three type-2 DGAT homologue genes for triacylglycerol production in the green microalga *Chlamydomonas reinhardtii*. J. Biotechnol., in press. doi:10.1016/j.jbiotec.2012.04.006.
27. **Leber R, Zinser E, Zellnig G, Paltauf F, Daum G.** 1994. Characterization of lipid particles of the yeast, *Saccharomyces cerevisiae*. Yeast **10**:1421–1428.
28. **Livak KJ, Schmittgen TD.** 2001. Analysis of relative gene expression data using real-time quantitative PCR and the 2(-Delta Delta C(T)) method. Methods **25**:402–408.

29. **Luo J, et al.** 2010. Histone h3 exerts a key function in mitotic checkpoint control. Mol. Cell. Biol. **30**:537–549.
30. **Ma H, Kunes S, Schatz PJ, Botstein D.** 1987. Plasmid construction by homologous recombination in yeast. Gene **58**:201–216.
31. **Merchant SS, et al.** 2007. The *Chlamydomonas* genome reveals the evolution of key animal and plant functions. Science **318**:245–250.
32. **Miege C, Marechal E.** 1999. 1,2-*sn*-Diacylglycerol in plant cells: product, substrate and regulator. Plant Physiol. Biochem. **37**:795–808.
33. **Miller R, et al.** 2010. Changes in transcript abundance in *Chlamydomonas reinhardtii* following nitrogen deprivation predict diversion of metabolism. Plant Physiol. **154**:1737–1752.
34. **Moellering ER, Benning C.** 2010. RNA interference silencing of a major lipid droplet protein affects lipid droplet size in *Chlamydomonas reinhardtii*. Eukaryot. Cell **9**:97–106.
35. **Molnar A, et al.** 2009. Highly specific gene silencing by artificial microRNAs in the unicellular alga *Chlamydomonas reinhardtii*. Plant J. **58**:165–174.
36. **Pazour GJ, Agrin N, Leszyk J, Witman GB.** 2005. Proteomic analysis of a eukaryotic cilium. J. Cell Biol. **170**:103–113.
37. **Rajakumari S, Daum G.** 2010. Multiple functions as lipase, steryl ester hydrolase, phospholipase, and acyltransferase of Tgl4p from the yeast *Saccharomyces cerevisiae*. J. Biol. Chem. **285**:15769–15776.
38. **Riekhof WR, Sears BB, Benning C.** 2005. Annotation of genes involved in glycerolipid biosynthesis in *Chlamydomonas reinhardtii*: discovery of the betaine lipid synthase BTA1Cr. Eukaryot. Cell **4**:242–252.
39. **Rietveld AG, Killian JA, Dowhan W, de Kruijff B.** 1993. Polymorphic regulation of membrane phospholipid composition in *Escherichia coli*. J. Biol. Chem. **268**:12427–12433.
40. **Rigaut G, et al.** 1999. A generic protein purification method for protein complex characterization and proteome exploration. Nat. Biotechnol. **17**: 1030–1032.
41. **Rochaix JD.** 1995. *Chlamydomonas reinhardtii* as the photosynthetic yeast. Annu. Rev. Genet. **29**:209–230.
42. **Rosenbaum JL, Witman GB.** 2002. Intraflagellar transport. Nat. Rev. Mol. Cell Biol. **3**:813–825.
43. **Rossak M, Schafer A, Xu N, Gage DA, Benning C.** 1997. Accumulation of sulfoquinovosyl-1-O-dihydroxyacetone in a sulfolipid-deficient mutant of *Rhodobacter sphaeroides* inactivated in sqdC. Arch. Biochem. Biophys. **340**:219–230.
44. **Roughan PG, Slack CR.** 1982. Cellular organization of glycerolipid metabolism. Annu. Rev. Plant Physiol. Plant Mol. Biol. **33**:97–132.
45. **Sandager L, et al.** 2002. Storage lipid synthesis is non-essential in yeast. J. Biol. Chem. **277**:6478–6482.
46. **Schneider JC, Roessler P.** 1994. Radiolabeling studies of lipids and fatty acids in *Nannochloropsis* (Eustigmatophyceae), an oleaginous marine alga. J. Phycol. **30**:594–598.
47. **Shen S, et al.** 2011. Tight regulation of diacylglycerol-mediated signaling is critical for proper invariant NKT cell development. J. Immunol. **187**: 2122–2129.
48. **Sherman F.** 1991. Getting started with yeast. Methods Enzymol. **194**:3–21.
49. **Siaut M, et al.** 2011. Oil accumulation in the model green alga *Chlamydomonas reinhardtii*: characterization, variability between common laboratory strains and relationship with starch reserves. BMC Biotechnol. **11**:7.
50. **Utsugi A, Kanda A, Hara S.** 2009. Lipase specificity in the transacylation of triacylglycerin. J. Oleo Sci. **58**:123–132.
51. **Wach A, Brachat A, Pohlmann R, Philippsen P.** 1994. New heterologous modules for classical or PCR-based gene disruptions in *Saccharomyces cerevisiae*. Yeast **10**:1793–1808.
52. **Wang ZT, Ullrich N, Joo S, Waffenschmidt S, Goodenough U.** 2009. Algal lipid bodies: stress induction, purification, and biochemical characterization in wild-type and starchless *Chlamydomonas reinhardtii*. Eukaryot. Cell **8**:1856–1868.
53. **Zhang M, Fan J, Taylor DC, Ohlrogge JB.** 2009. DGAT1 and PDAT1 acyltransferases have overlapping functions in *Arabidopsis* triacylglycerol biosynthesis and are essential for normal pollen and seed development. Plant Cell **21**:3885–3901.